Experiment and Simulation for Controlling Propagation Direction of Hydrofracture By Multi-Boreholes Hydraulic Fracturing

Chenpeng Song[1, 2], Yulong Chen[3, *] and Jiehao Wang[2, *]

Abstract: Hydraulic fracturing has been applied to enhance CBM production and prevent gas dynamical hazard in underground coal mines in China. However, affected by in situ stress orientation, hydrofracture can hardly continuously propagate within coal seam but may easily extend to the adjacent roof-floor strata, causing ineffective permeability enhancement in coal seam and increasing the risk of gas transfinite during mining coal. Thus, it is very necessary to artificially control the propagation direction of hydrofracture and make it well-aligned in large scale in coal seam. In this study, a method for controlling propagation direction of hydrofracture by multi-boreholes is investigated by theoretical analysis, laboratory experiment and numerical simulation. And this is followed by an on-site test in an underground coal mine to verify this method. Firstly, stress intensity factor at the hydrofracture tip is analyzed where pore pressure is taken into consideration. Results show that the pore pressure is able to increase the stress intensity factor and reduce hydrofracture propagation pressure. Based on this, a method of hydraulic fracturing using multi-boreholes to control hydrofracture direction is proposed. Afterwards, laboratory experiments are conducted to explore the impact of pore pressure on hydrofracture propagation. The experimental results agree with the theoretical analysis very well. Later on, a series of numerical simulations are performed to examine the influence of principal stress difference, the angle between assistance drillholes and the maximum principal stress, and the fluid pressure of the assistance drillholes on hydrofracture propagation. Finally, an on-site test in an underground coalmine is practiced where this proposed method is used to enhance the CBM production. Results show the scope of the hydro-fracture resulting from the multi-boreholes hydraulic fracturing method increases 2.7 times compared with that of conventional hydraulic fracturing. And gas production rate also increases 4.1 times compared with that of conventional hydraulic fracturing and 12.3 times compared with direct borehole extraction without fracturing.

Keywords: Coalbed methane, underground coalmine, hydraulic fracturing, pore pressure, multi-borehole.

[1] National and Local Joint Engineering Laboratory of Traffic Civil Engineering Materials, Chongqing Jiaotong University, Chongqing, 400074, China.

[2] Department of Energy and Mineral Engineering, EMS Energy Institute and G3 Center, Pennsylvania State University, University Park, PA 16802, USA.

[3] School of Energy and Mining Engineering, China University of Mining and Technology, Beijing, 100083, China.

[*] Corresponding Authors: Yulong Chen. Email: chenyulong@cumtb.edu.cn;

Jiehao Wang. Email: jiehao.wang@psu.edu.

1 Introduction

CBM (coalbed methane) has become an important source of energy in China due to its abundance. Among 17.3 billion m^3 of total CBM production of China in 2016, more than 70% of CBM was recovered at underground coal mines and only 26% of CBM was from ground-based extraction [Li, Lau and Huang (2017); Qin, Moore, Shen et al. (2018); Tang, Yang, Zhai et al. (2018)]. This is mainly due to the fact that the geological conditions of most CBM reservoirs are quite complex and cannot meet the requirements for ground-based development. Therefore, a large part of CBM output is extracted through underground boreholes before mining coal resource [Song and Elsworth (2018)]. Meanwhile, gas pre-extraction is also a primary measure for gas-disaster prevention in underground coalmines [Lu, Liu, Li et al. (2010); Wang, Wu, Wang et al. (2017)]. Maximizing the gas extraction area of borehole and the gas extraction rate of borehole is a very important issue. In recent ten years, the hydraulic fracturing in underground coal mine has been proposed and applied to enhance CBM output and prevent gas dynamical hazard. In this treatment, highly pressurized fluid is used to crack the formation and drive the fractures propagation via the borehole which is usually drilled from the coal-floor roadway to coal seam [Wang, Wu, Wang et al. (2017)]. The field test by our research team has indicated that the average borehole's extraction rate after hydraulic fracturing can be increased by 3-5 times compared with no treatment borehole. However, since the thickness of coal seam is much less than the oil-gas reservoir and the propagation of hydrofracture is affected by the in-situ stress orientation, hydrofracture can easily extend into the roof-floor strata, causing ineffective permeability enhancement in coal seam and the roof-floor strata difficult to be supported while mining coal in later phase [Song, Lu, Tang et al. (2016)]. And more importantly, the ineffective permeability enhancement limits the amount of gas that can be drained, greatly increasing the risk of gas transfinite and even gas outburst during mining coal. Thus, it is very necessary to artificially control the propagation direction of hydrofracture and make it well-aligned in large scale in coal seam.

For ground-based wells, the current hydro-fracture control method mainly uses directional drilling technology in which well track is effectively controlled by means of special down hole tools and measuring instruments. This method is able to direct the drill towards the preset target through particular direction, which can substantially increase oil-gas production and reduce drilling cost [Lu, Song, Jia et al. (2015); Surjaatmadja, Grundmann, McDaniel et al. (2007)]. However, for hydraulic fracturing at underground coalmines, directional drilling technology cannot be used due to the limitation of tunnel space and the conditions of coal seams. And since that the other main CBM production countries (USA, Australia, Canada, etc.) mainly use ground-based extraction [Cooper (1994)], there is no available method can be referred to. Therefore, finding a method to control hydrofracture propagation in underground coalmines is an important scientific and technical issue to significantly increase CBM production and prevent of mine gas disasters in China.

This research is focused on the multi-boreholes hydraulic fracturing for controlling direction of hydrofracture propagation based on pore-pressure gradient. Firstly, it starts with a theoritical analysis to get the stress intensity factor of hydrofracture tip where pore pressure is involved. A method for controlling propagation direction of hydrofracture was proposed according to the above analysis. Next, the feasibility of this method was

investigated through a series of laboratory fracturing experiments and numerical simulations. Finally, the method was tested in an underground coalmine, and the propagation range of hydrofractures and gas drainage data were analyzed and compared with conventional technology.

2 The criterion of hydrofracture propagation while considering pore pressure

Due to the poroelasticity effect, the pre-existing field of pore pressure could have a significant influent of the propagation direction of a hydraulic fracture. However, this effect has been fully understood by previously developed models. In this part, a criterion of hydrofracture propagation is discussed where the effect of pore pressure is considered. Consider an infinite flat plate subjected to far field in-situ stresses σ_1 and σ_3 ($\sigma_1 > \sigma_3$), which contains a fracture with length being 2L and angle between the fracture and σ_1 being α (see Fig. 1). A fluid pressure P_w is applied within the fracture. A uniform pore pressure P_0 is applied in the matrix surrounding the fracture. According to the superposition principle of stress intensity factors, the stress intensity factor at the fracture tip are superposited by the far-field in-situ stress, fracture internal fluid pressure P_w and external pore pressure P_0.
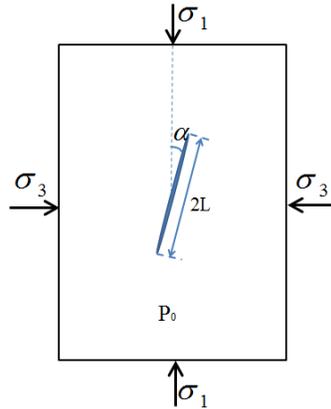
Figure 1: Hydro-fracture model. A fracture of length 2*L* is subjected to the in-situ stresses, σ_1 and σ_3, internal fluid pressure, P_w, and external pore pressure, P_0. α is the angle between the fracture and σ_1

Hydraulic fractures are usually assumed to be created by purely tensile stress, i.e., they are type I fractures. However, when they are not aligned with the in-situ stresses, shear stress might also contribute to the propagation of hydraulic fractures. Therefore, mode I and mode II mixed fractures are considered in this study. According to the theory of linear elastic fracture mechanics, type I and type II crack tip stress intensity factors are respectively expressed as follows:

$$K_I = \sigma_\alpha \sqrt{\pi L} \tag{1}$$

$$K_{II} = \tau_\alpha \sqrt{\pi L} \tag{2}$$

where K_I and K_{II} are type I and type II crack stress intensity factors, respectively; σ_α and τ_α are the normal stress and shear stress on the crack surface, respectively.

Under separate actions of above three forces, type I and type II crack stress intensity factors on the crack surface can be respectively written as follows:

Under the action of far-field in-situ stresses:

$$K_I' = -(\frac{\sigma_1 + \sigma_3}{2} - \frac{\sigma_1 - \sigma_3}{2} \cos 2\alpha) \sqrt{\pi L} \tag{3}$$

$$K_{II}' = \frac{\sigma_1 - \sigma_3}{2} \sin 2\alpha \sqrt{\pi L} \tag{4}$$

Under the action of fluid pressure P_w within the crack:

$$K_I'' = P_w \sqrt{\pi L} \tag{5}$$

$$K_{II}'' = 0 \tag{6}$$

Under the action of pore pressure, the stress intensity factors at the crack tip are as follows [Cherepanov (2009); Detournay, Cheng, Roegiers et al. (1989)]:

$$K_I''' = \frac{1 - 2\nu}{\pi(1-\nu)} P_0 \sqrt{\pi L} \tag{7}$$

$$K_{II}''' = 0 \tag{8}$$

Superposing the crack tip stress intensity factors resulting from far-field in-situ stress, water pressure and pore pressure, the stress intensity factors can be written as

$$K_I = K_I' + K_I'' + K_I''' = (P_w - \frac{\sigma_1 + \sigma_3}{2} + \frac{\sigma_1 - \sigma_3}{2} \cos 2\alpha + \frac{1 - 2\nu}{\pi(1-\nu)} P_0) \sqrt{\pi L} \tag{9}$$

$$K_{II} = K_{II}' + K_{II}'' + K_{II}''' = \frac{\sigma_1 - \sigma_3}{2} \sin 2\alpha \sqrt{\pi L} \tag{10}$$

The propagation criterion of type I-II hydrofracture can be expressed as the following formula:

$$K_I + K_{II} = K_{IC} \tag{11}$$

where K_{IC} is the fracture toughness of type I.

Substituting Eqs. (9) and (10) into Eq. (11), the fluid pressure required for crack propagation is as follows:

$$P_w = \frac{K_{IC}}{\sqrt{\pi L}} - \frac{\sigma_1 - \sigma_3}{2} (\sin 2\alpha + \cos 2\alpha) + \frac{\sigma_1 + \sigma_3}{2} - \frac{1 - 2\nu}{\pi(1-\nu)} P_0 \tag{12}$$

As described in Eq. (12), when a pore pressure exists around the crack tip, the fluid pressure

required for crack propagation will decrease by $\dfrac{1-2\nu}{\pi(1-\nu)}P_0$. If there is a pore pressure gradient field in porous material, hydrofracture will tend to propagate in the direction of high pore pressure in order to reduce the fluid pressure required for crack propagation, i.e., the fracture will propagate following a path where the least energy is dissipated. If the pore pressure applied is bigger, the hydraulic fracture deflection tendency is expected to be more obvious. Therefore, we propose a method to guide the direction of hydrofacture in underground coal mine. Namely, several assistant boreholes are drilled on both sides of the hydraulic fracturing borehole along the preset crack propagation path, as shown in Fig. 2. Before hydraulic fracturing, fluid is injected into assistant boreholes and the pressure is maintained for a certain peroid of time to increase the pore pressure and form a continuous strap-shaped higher pore pressure area around the hydraulic fracturing borehole, and this will guide the hydraulic fracture to propagate along the preset direction. In the next section, a series of laboratory experiments were conducted to test this proposed method.
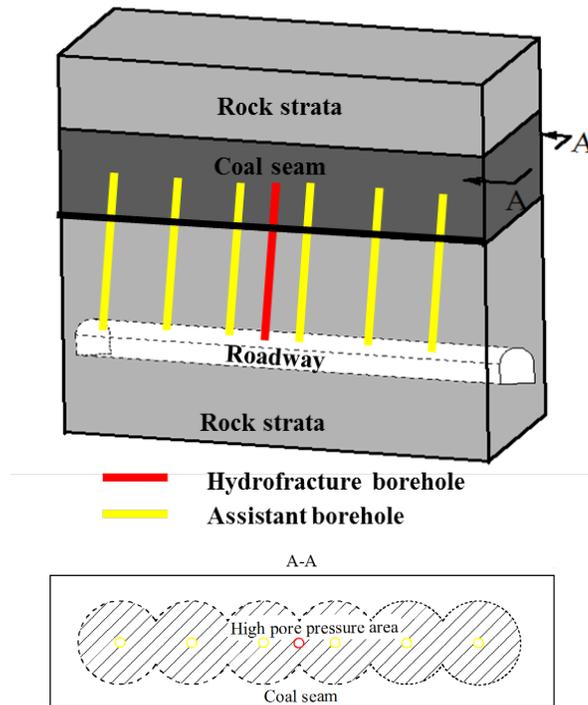
Figure 2: Multi-boreholes hydraulic fracturing. Several assistant boreholes (shown in yellow color) are drilled on both sides of the hydraulic fracturing borehole (shown in red color) along the preset crack propagation path

3 Experimental study on pore pressure influencing hydrofracture

In this section, we conducted experiments to investigate the influence of pore pressure gradient on hydrofracture propagation. As shown in Fig. 3, the specimen is a 100 mm×200

mm×100 mm cuboid sandstone, where two holes will be drilled. No. 1 hole is the hydraulic fracturing hole and No. 2 hole is the assistant hole. The use of sandstone samples instead of coal samples is mainly due to the following two reasons: (1) it is difficult to prepare coal samples with that big scale; (2) the heterogeneity of coal may affect experimental results. The purpose of the experiments is to demonstration the ability of pore pressure to guide the direction of the hydraulic fractures. Admittedly the coal seams are typically naturally fractured, but involvement of the natural fractures in the samples could complicate the experimental results and make it difficult to isolate the impact of the pore pressure from that of the heterogeneity. Although it is somehow oversimplified by using sandstone instead of coal, the experimental results should be adequate to deliver some fundamental and important considerations on utilizing pore pressure to control the direction of fracture propagation. The schematic of experimental apparatus is shown in Fig. 4. Only a constant axial stress of 10 MPa is applied in the vertical direction to control the hydrofracture to propagate in the vertical direction. Before hydraulic fracturing the No. 1 hole, water is injected into the No. 2 hole and a constant pressure will be maintained for 5 mins, resulting in partial high pore pressure around it. And then, No.1 hole is pressurized at a constant flow rate until hydrofractures are formed.
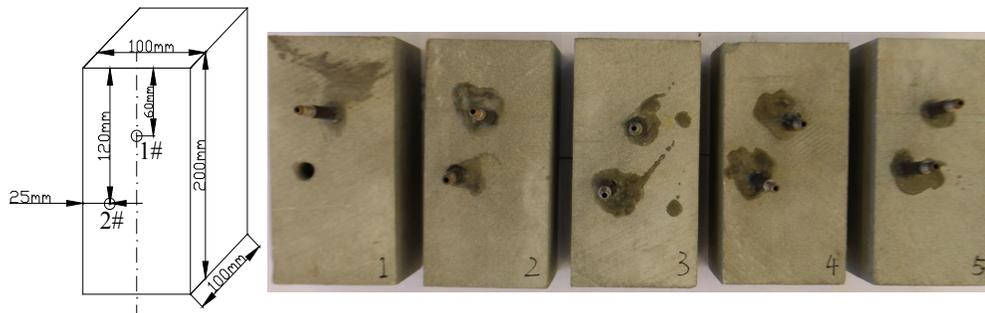
Figure 3: Experimental specimens. The specimen is a 100 mm×200 mm×100 mm cuboid sandstone, where two holes will be drilled. No. 1 hole is the hydraulic fracturing hole and No. 2 hole is the assistant hole
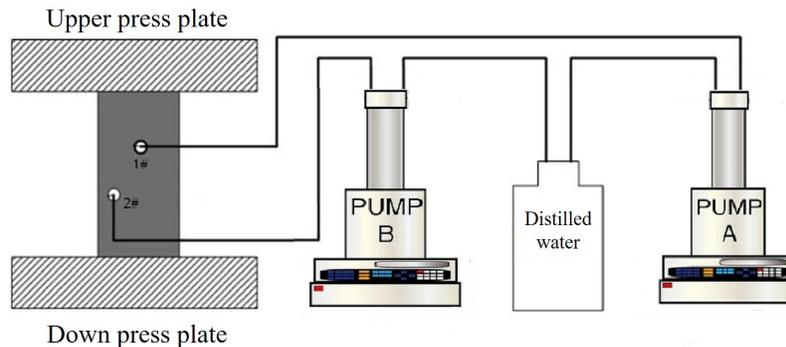
Figure 4: Schematic of experimental apparatus

A total of five groups of experiments with different pressures in No. 2 hole were conducted, as listed in Tab. 1. The resulting hydro-fractures of the five groups are shown

in Fig. 5. When No. 2 hole is not applied with water pressure (Group 1), the crack extends along the direction of maximum principle stress, i.e., it extends in the vertical direction. In the 2-5 groups with constant water pressure being applied in No. 2 hole, the pore pressure gradient is formed around the No. 2 hole resulting from the infiltration of water into the rock matrix. When the water pressure in the No. 2 hole increases, the asymmetry of the pore pressure gradient is more obvious. Therefore, the crack gradually turns to the direction of the No. 2 hole. This can also be qualitatively explained by the theoretical analysis, i.e., Eq. (12). The resulting fracture tend to propagate along the path which dissipates the least energy. With a larger pore pressure, the required hydraulic pressure to extend the fracture will be reduced and thus consumes less energy. Therefore, as pressure increases in the No. 2 hole, the direction of the fracture turns to it gradually. In next section, we will conduct further analysis on multi-boreholes hydraulic fracturing through numerical simulations.

Table 1: Axial pressure and pressures in No. 2 holes for the 5 groups

Group Number	Axial Pressure/MPa	#2 Pressure/MPa
1	10	0
2	10	2
3	10	4
4	10	6
5	10	8

Figure 5: Resulting hydro-fractures with different pressures in No. 2 holes. The crack gradually turns to the direction of the No. 2 hole as the water pressure in the No. 2 hole increases

4 Numerical simulation

Based on the theoretical and experimental analysis above, there are three main factors influencing crack propagation direction in the multi-boreholes hydraulic fracturing, including in-situ stress difference, the angle between the assistant borehole and maximum principal stress, as well as the pressure in the assistant borehole. In this section, we use

the coupling system of flow & solid in rock failure process analysis (RFPA2D-Flow) to conduct numerical simulation analysis on the influence of three factors [Tang, Tham, Lee et al. (2002); Yang, Tham, Tang et al. (2004)].

RFPA2D-Flow is based on the following basic assumptions:

① The seepage process meets Biot consolidation theory and the modified Terzaghi effective stress principle.

② The rock microscopic representative elementary volumes (REVs) are elastic and brittle, and have residual strength. The mechanical behavior of REVs can be described with elastic-failure theory, and the maximum tensile strain criterion and Mohr-Coulomb criterion are used as the failure threshold.

③ The permeability of REVs in elastic state evolves according to permeability-stress models and increases dramatically after damage occurs.

④ Rock is heterogeneous and the mechanical parameters of REVs (elastic modulus and strength) meet the Weibull distribution.

The governing equations can be written as follows [Tang and Kou (1998); Xu, Tang, Yang et al. (2006)]:

Equilibrium equation $\sigma_{ij,j} + \rho X_j = 0$ $\qquad (i, j = 1,2,3)$ (13)

Strain-displacement relation $\varepsilon_{ij} = \dfrac{(u_{i,j} + u_{j,i})}{2}$ $\qquad \varepsilon_v = \varepsilon_{11} + \varepsilon_{22} + \varepsilon_{33}$ (14)

Constitutive equation $\sigma_{ij}' = \sigma_{ij} - \alpha p \delta_{ij} = \lambda \delta_{ij} \varepsilon_v + 2G\varepsilon_{ij}$ (15)

Seepage equation $K\nabla^2 p = \dfrac{1}{Q}\dfrac{\partial p}{\partial t} - \alpha \dfrac{\partial \varepsilon_v}{\partial t}$ (16)

Permeability-stress coupling equation $K(\sigma, p) = \xi K_0 e^{-\beta(\sigma_{ij}/3 - \alpha p)}$ (17)

In which σ_{ij} is the stress; ρ is the physical density of fluid; ε_v and ε_{ij} are the bulk strain and strain, respectively; δ is the Kronecker constant; Q is the Biot constant; G and λ are the shear modulus and the Lame coefficient; ∇^2 is the Laplace operator; K_0 and K are respectively the initial value of permeability coefficient and permeability coefficient; P is the pore pressure; ξ, α, β are respectively jump rate of permeability coefficient, pore pressure coefficient, and coupling coefficient. Detailed algorithm to solve this equation system can be found in Tang et al. [Tang, Tham, Lee et al. (2002); Yang, Tham, Tang et al. (2004)].

When the stress or strain state of a REV satisfies a given failure threshold, damage occurs and the elastic modulus decreases with the damage evolution: $E = (1 - D)E_0$, where D is the damage variable and E_0 is the initial elastic modulus. A constitutive law defining *D* is given in Zhang et al. [Zhang, Ma, Wu et al. (2018)], and therefore is omitted here for brevity.
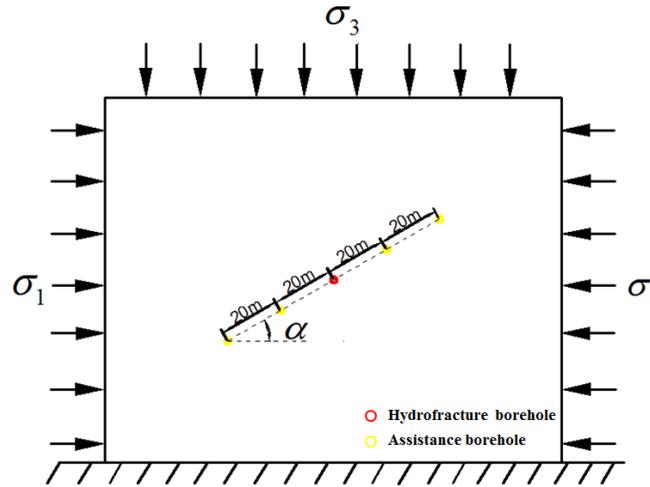
Figure 6: Geometry and loading conditions of the model

The geometries and loading conditions of the model are defined as shown in Fig. 6. A total of five boreholes are arranged on a straight line and equally spaced with a length of 20 m. The center borehole is hydraulic fracturing borehole and the other boreholes are assistant boreholes. The maximum horizontal principal stress is applied horizontally, and the minimum horizontal principal stress is applied vertically. Since that the angle α between the connecting line of the boreholes and the maximum principal stress is different, the size of the model geometry is slightly different. The mechanical properties of coal seam are shown in Tab. 2. The values of the three above-mentioned controlling factors are shown in Tab. 3, i.e., the in-situ stress, the value of angle α and the pressure in the assistant boreholes. In the assistant boreholes, a constant water pressure P_0 as shown in Tab. 3 is applied in advance. The water pressure applied in the hydraulic fracturing borehole is increased by 0.2 MPa per step until unstable fracture propagation occurs. The Weibull distribution parameter is taken as 5 to represent the heterogeneity of the coal rock in this study.

Table 2: The mechanical parameters of coal seam

Mechanical parameter	value	Mechanical parameter	value
Elasticity modulus/MPa	7000	Friction angle	30°
Compression strength/MPa strength/MPa	20	Permeability coefficient/(m/d)	0.05
Tensile strength/MPa	1.5	Pore water pressure coefficient after damage	1
Poisson ratio	0.35	Pore water pressure coefficient	0.6

Table 3: The values of the three controlling factors used in the simulations

Group Number	α	σ_1 / MPa	σ_3 / MPa	P_0 / MPa
1	15°	12	10	6
2	15°	12	10	10
3	15°	16	10	6
4	15°	16	10	10
5	30°	12	10	6
6	30°	12	10	10
7	30°	16	10	6
8	30°	16	10	10
9	45°	12	10	6
10	45°	12	10	10
11	45°	16	10	6
12	45°	16	10	10
13	60°	12	10	6
14	60°	12	10	10
15	60°	16	10	6
16	60°	16	10	10

Fig. 7 shows the results of crack propagation. The background color shows the pore pressure distribution with the red area representing high pore pressure and the blue area representing low pore pressure. It can be seen that, when angle α increases, the hydrofracture tends to propagate along the direction of the maximum principal stress, and the guiding ability of the assistant boreholes gradually decreases. At the same time, the hydro-fracture propagation path becomes more zigzagged, and there are more branch cracks formed around the main fractures. In addition, as the water pressure in the assistant boreholes increases, the asymmetric trend of pore pressure gradient becomes more obvious and the guidance ability of the assistant borehole increases. The control ability of the assistant borehole is further enhanced by the small difference in in-situ stresses. Note that, when the angle α is 0, it is obvious that the hydraulic fractures will propagate along the direction exactly perpendicular to the minimum stress, which is favored by both of the in-situ stresses and the guidance of the assistant boreholes. And when the angle α is 90 degree, a hydraulic fracture perpendicular to the minimum stress is also expected, considering the resulting symmetric distribution of the pore pressure and the ineffective guidance of the assistant boreholes at the angle of 60 degree. The numerical simulation results further verify the theoretical analysis and experimental results. Based on the findings above, we conducted a field experiment in the underground coal mine to further test the proposed method.

$\alpha = 15°, \triangle\sigma = 2MPa, P_0 = 6MPa$

$\alpha = 15°, \triangle\sigma = 2MPa, P_0 = 10MPa$

$\alpha = 15°, \triangle\sigma = 6MPa, P_0 = 6MPa$

$\alpha = 15°, \triangle\sigma = 6MPa, P_0 = 10MPa$

$\alpha = 30°, \triangle\sigma = 2MPa, P_0 = 6MPa$

$\alpha = 30°, \triangle\sigma = 2MPa, P_0 = 10MPa$

$\alpha = 30°, \triangle\sigma = 6MPa, P_0 = 6MPa$

$\alpha = 30°, \triangle\sigma = 6MPa, P_0 = 10MPa$

$\alpha = 45^{\circ}, \triangle\sigma = 6MPa, P_0 = 6MPa$

$\alpha = 45^{\circ}, \triangle\sigma = 2MPa, P_0 = 10MPa$

$\alpha = 45^{\circ}, \triangle\sigma = 2MPa, P_0 = 6MPa$

$\alpha = 45^{\circ}, \triangle\sigma = 6MPa, P_0 = 10MPa$

$\alpha = 60^{\circ}, \triangle\sigma = 6MPa, P_0 = 6MPa$

$\alpha = 60^{\circ}, \triangle\sigma = 2MPa, P_0 = 10MPa$
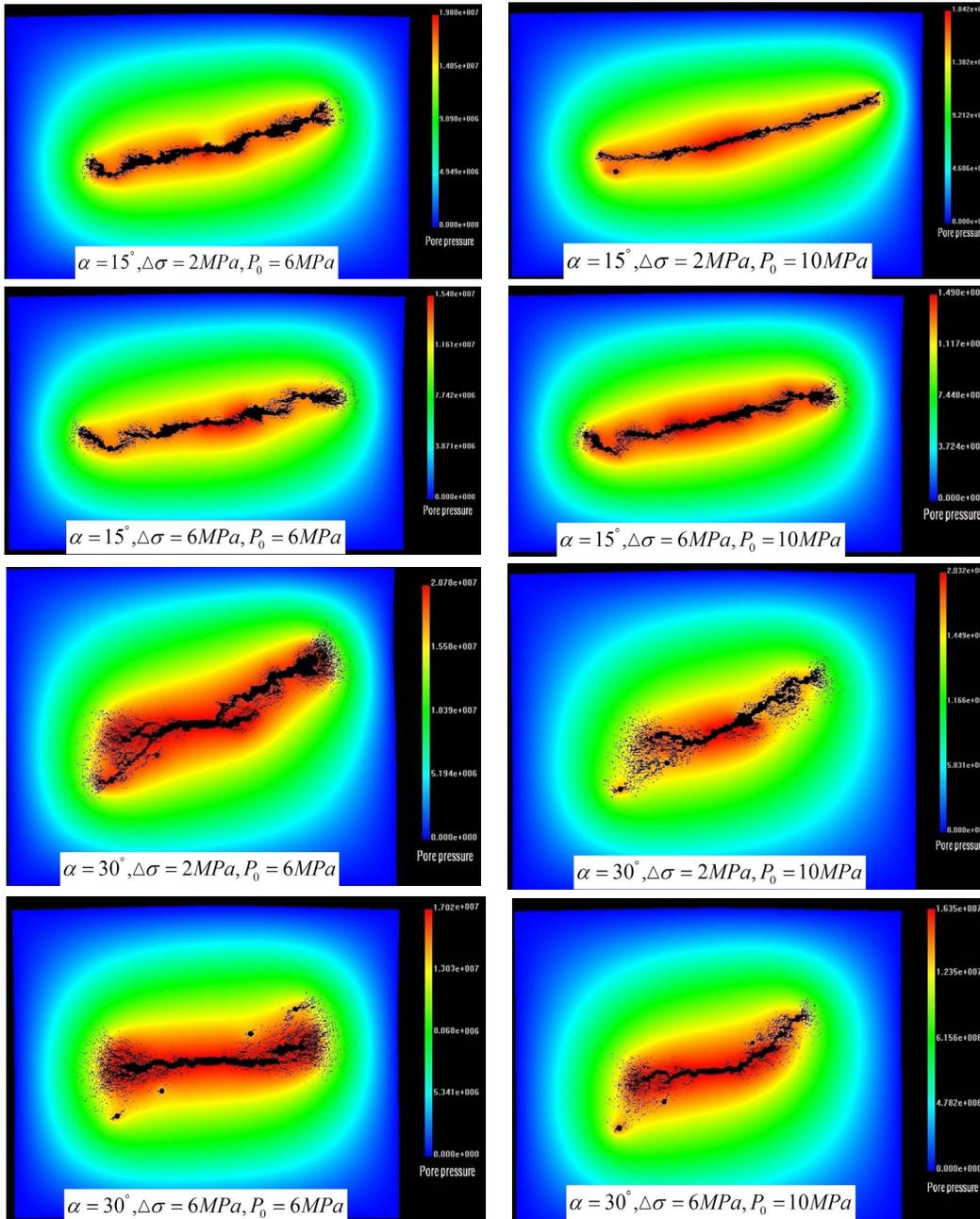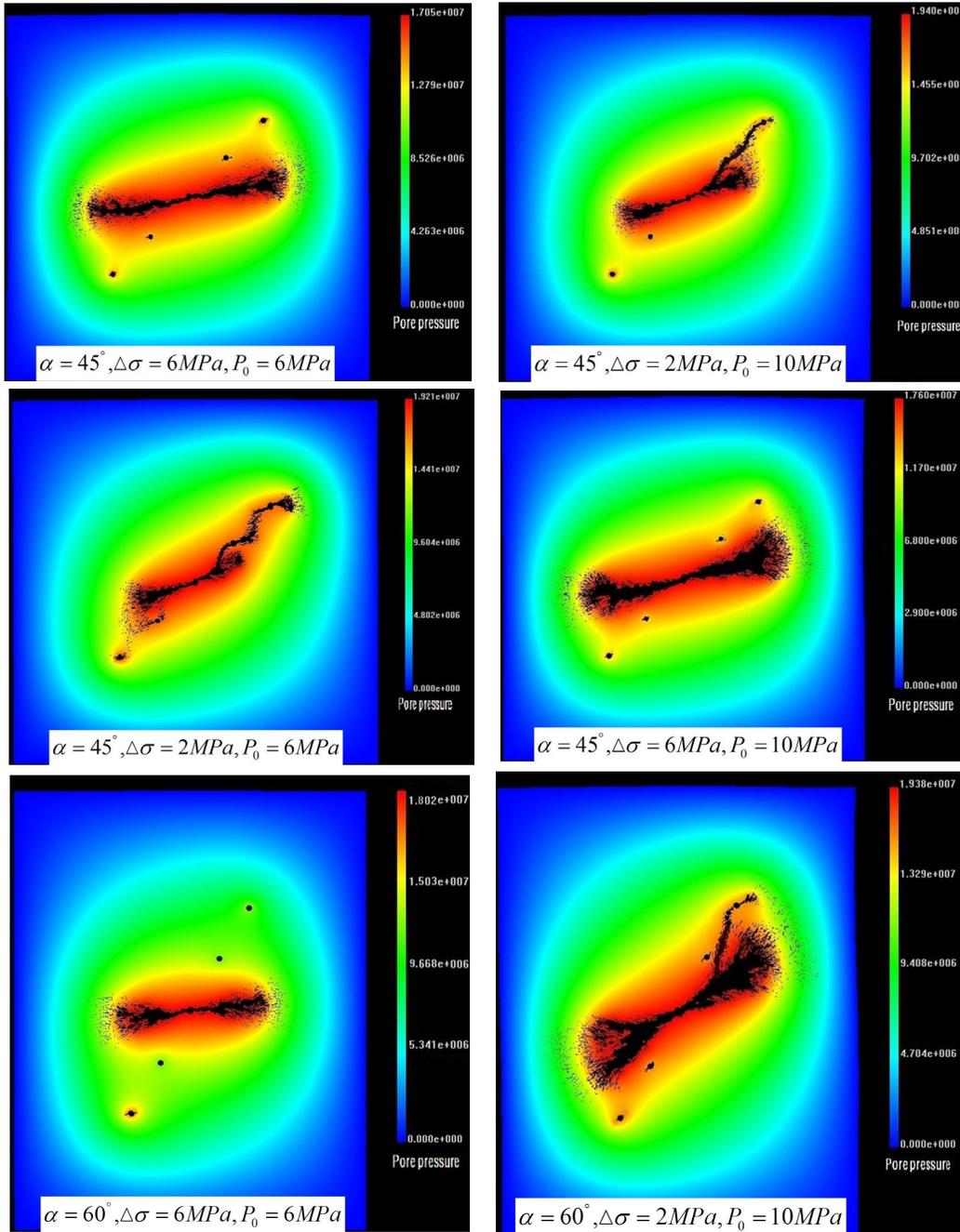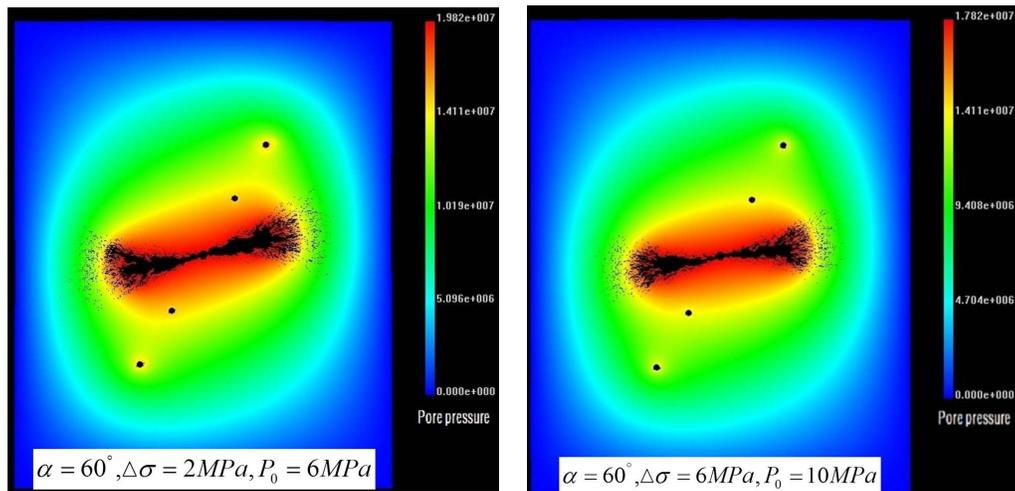
Figure 7: Hydrofracture propagation results. The black color represents damaged REVs, while the background color represents the distribution of pore pressure

5 Field test

In this section, an underground experiment was conducted in the Fengchun coal mine of Chongqing Songzao mining area to examine the applicability of multi-boreholes hydraulic fracturing in field and compare it with conventional hydraulic fracturing methods in terms of crack extension and CBM production.

5.1 Overview of hydraulic fracturing area

The test site is located at S11203 head entry. And the coal seam for hydraulic fracturing is M8 coal seam. The average thickness of M8 coal seam is 1.83 m, the angle of inclination is 16° and the buried depth is 525 m.

The plan view and cutaway view of the construction area and borehole layout are shown in Fig. 8. The boreholes are located at S11203 head entry. The spacing between the six drilled assistant boreholes is 20 m. The end point of all boreholes is at the same level and the dip angle of all boreholes is approximately perpendicular to the coal seam. A single hydrofracture borehole test is also arranged at S11203 head entry to compare with the multi-boreholes hydraulic fracturing. And the parameters of borehole are identical to the multi-boreholes hydraulic fracturing. The two experimental sites are separated by 300 m to ensure that there is no mutual influence.
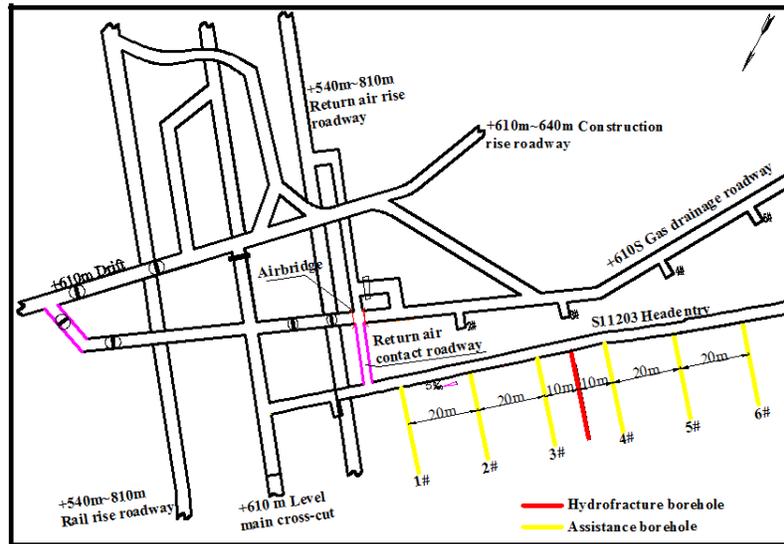
Figure 8: The plan view of hydraulic fracturing area.
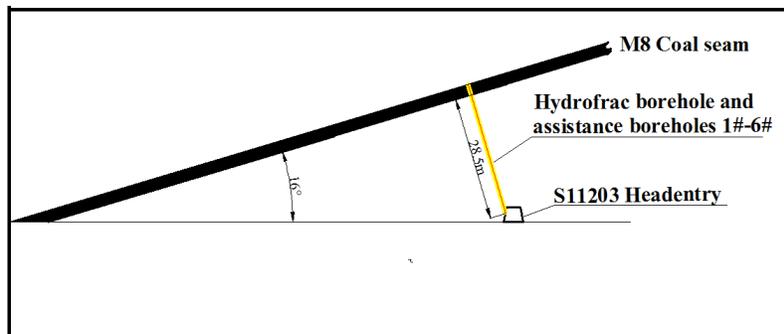
Figure 9: The cutaway view of borehole layout

5.2 Field test process and phenomenon analysis

Riverfrac treatment is used in this experiment. In multi-boreholes hydraulic fracturing test. The assistant boreholes are first loaded with 20 MPa water pressure for 20 mins, and then the hydrofracture drillhole is injected high pressure water for 120 mins where the pump works in a constant-pressure mode. Note that this constant pressure is set as 40 MPa which might be relatively larger than the breakdown pressure, thus the pressure in the hydrofracture drillhole can hardly reach 40 MPa but oscillates around a lower pressure. Since that the resultant fractures are difficult to be visualized [Wang and Elsworth (2018)], a small amount of surfactant is added in the fracturing fluid in order to detect the range of crack propagation after treatment is completed. The histories of pump pressure and flow rate during the hydraulic fracturing process are shown in Fig. 10. In the conventional hydraulic fracturing test, the hydro-fracture borehole is also pressurized for 120 mins, and the histories of the pump pressure and flow rate are shown in Fig. 11.
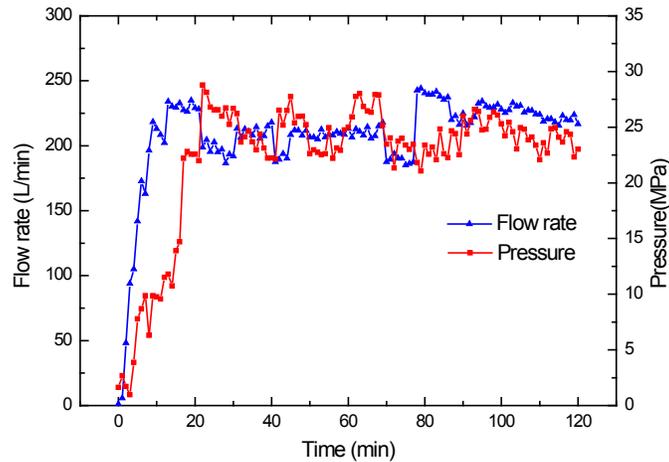
Figure 10: Histories of pumping pressure (red line) and flow rate (blue line) of multi-borehole fracturing
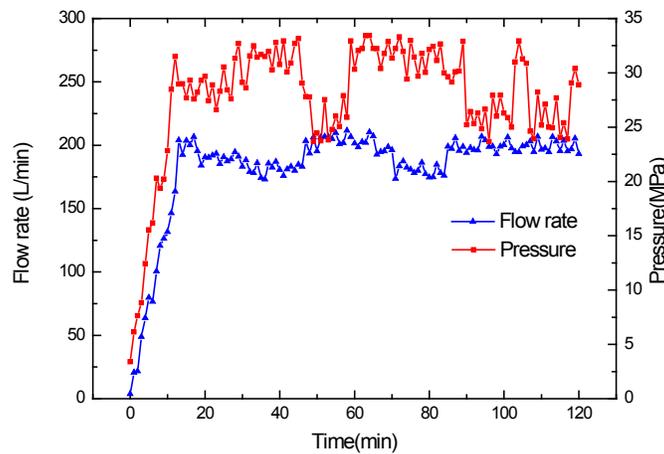
Figure 11: Histories of pumping pressure (red line) and flow rate (blue line) of conventional fracturing

It can be seen from Figs. 10 and 11 that the fracture propagation pressure of multi-boreholes hydraulic fracturing and conventional hydraulic fracturing are 23-27 MPa and 25-33 MPa, respectively. It is mainly due to that, in the multi-boreholes hydraulic fracturing, the higher pore pressure around the assistant boreholes reduces the pumping pressure required for the crack propagation, as indicated by Eq. (12). The injection flow rate in the multi-boreholes hydraulic fracturing is higher than that in the conventional hydraulic fracturing. This may result from that, combined the results from numerical simulation, the fractures created by the multi-borehole fracturing are more tortuous and have more branches around them compared with those generated by the conventional fracturing. As a result, those complex fractures offer high-conductivity channels for the injected fracturing fluid.

5.3 Dimension of the resulting hydro-fractures

After multi-boreholes hydraulic fracturing test, six assistant boreholes are immediately drained. Foamed water, due to the addition of surfactant in the fracturing fluid, is found in all assistant boreholes except the No. 6 one, implying that the effective length of hydraulic fracturing is more than 80 m. Note that the surfactant is used only as an indicator to characterize the length of the induced fracture, and thus its concentration is not measured.

The dimension of the fracturing resulting from the conventional hydraulic fracturing is decided by testing the moisture content of the coal. Four inspection holes were drilled every 10m along the direction of the roadway on each side of the hydro-fracture borehole. The parameters of inspection holes are identical to the borehole of hydraulic fracturing. The test results are listed in Tab. 4 and it is apparent that the length of the hydro-fracture is ~30 m. Meanwhile, it was found that the rock mass at the top of S11203 head entry is wetted after the test, which indicates that some of the hydrofractures have extend into the floor strata. Measurement of the moisture content is performed right after the hydraulic fracturing job which prevents the fracturing water from diffusing a significant length. Therefore, given the considerably different moisture content at those inspection holes, the evaluation of the fracture length using this method should be reliable and effective. Although there are some other more sophisticated techniques to characterize the resulting fracture, such as microseismic monitoring, they are relatively costly when applied in a large scale.

Table 4: The moisture content of coal

No.	Moisture content /%	Distance from hydrofracture borehole
original content	0.47-0.65	\
1#	6.83	Left 10 m
2#	5.66	Left 20 m
3#	0.53	Left 30 m
4#	0.67	Left 40 m
5#	5.28	Right 10 m
6#	0.67	Right 20 m
7#	0.54	Right 30 m
8#	0.61	Right 40 m

5.4 Comparison of CBM production

In multi-boreholes hydraulic fracturing, the hydrofracture borehole and six assistant boreholes are used for CBM extraction. In conventional hydraulic fracturing, the hydro-fracture borehole and eight inspection boreholes are used to extract CBM. The comparison of CBM extraction in both methods during the beginning 33 days is shown in Fig. 12. The average production rate per borehole of multiple-boreholes hydraulic fracturing is 0.037 m^3/min, while that of conventional hydraulic fracturing is 0.009

m^3/min. For the boreholes in S11203 head entry where hydraulic fracturing is absent, the average extraction flow rate of CBM is only 0.003 m^3/min during the beginning 33 days. After adopting multi-boreholes hydraulic fracturing method, compared with conventional hydraulic fracturing and borehole drainage without fracturing, the gas production rate is increased by 4.1 times and 12.3 times, respectively. Therefore, CBM production rate can maintain at a high level by using multi-boreholes hydraulic fracturing. In addition, CBM production rate of conventional hydraulic fracturing almost decreases to the level of borehole drainage without fracturing after 14 days. Therefore, the multi-boreholes hydraulic fracturing method can achieve large-scale and directional expansion of crack and effective increase of gas production.
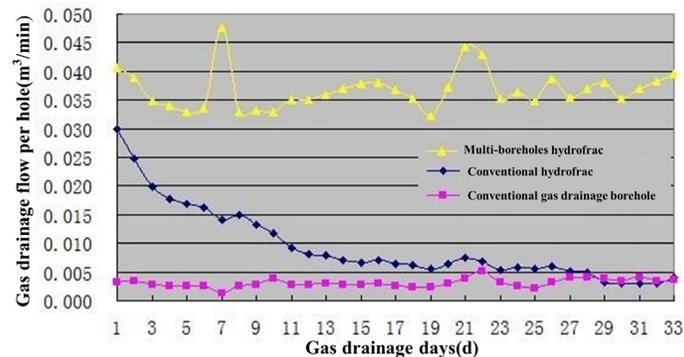
Figure 12: CBM production rate of multi-borehole hydraulic fracturing (yellow line), conventional hydraulic fracturing (blue line) and direct borehole drainage without fracturing (pink line)

6 Conclusions

This paper studies the effect of pore pressure on hydrofracture propagation. The pore pressure is able to increase the stress intensity factors of crack tip and reduce hydro-fracture propagation pressure. Based on this, a method of hydraulic fracturing using multi-borehole is proposed which is able to control hydrofracture direction based on pore pressure gradient. Several assistant boreholes are drilled on both sides of the hydraulic fracturing borehole along the preset crack propagation direction. Before hydraulic fracturing, water is injected into the assistant boreholes and pressure is maintained for a certain period of time to increase the pore pressure around the hydraulic fracturing borehole, which is able to guide the hydraulic fracture to propagate along the preset direction.

In the multi-boreholes hydraulic fracturing method, there are three main factors influencing crack propagation direction, including in-situ stress difference, the angle between assistant borehole and the maximum principal stress, and the fluid pressure in the assistance boreholes. When the angle increases, the hydrofracture tends to propagate along the direction of the maximum principal stress and the hydro-fracture becomes more zigzagged, and there are more branch cracks formed around the main fractures. As the constant water pressure applied in assistant boreholes increases, the ability of this method

to control hydrofracture propagation direction decreases. And this ability is further limited by a large principle stress difference.

Field experiment in underground coalmine shows that the length of the resulting hydro-fracture of multi-borehole hydraulic fracturing is ~80 m, while that of the conventional hydraulic fracturing is only ~30 m. Compared with the conventional hydraulic fracturing and direct extraction without fracturing, the gas production rate of the multi-boreholes hydraulic fracturing increases 4.1 times and 12.3 times during the beginning 33 days, respectively.

References

Cherepanov, G. P. (1979): *Mechanics of Brittle Fracture*. McGraw-Hill Press.

Cooper, G. A. (1994): Directional drilling. *Scientific American*, vol. 270, no. 5, pp. 82-87.

Detournay, E.; Cheng, A. D.; Roegiers, J. C.; McLennan, J. D. (1989): Poroelasticity considerations in in situ stress determination by hydraulic fracturing. *International Journal of Rock Mechanics and Mining Sciences & Geomechanics Abstracts*, vol. 26, no. 6, pp. 507-513.

Li, H.; Lau, H. C.; Huang, S. (2017): Coalbed methane development in China: engineering challenges and opportunities. SPE/IATMI Asia Pacific Oil & Gas Conference and Exhibition. *Society of Petroleum Engineers*, SPE-186289-MS.

Lu, Y.; Liu, Y.; Li, X.; Kang, Y. (2010): A new method of drilling long boreholes in low permeability coal by improving its permeability. *International Journal of Coal Geology*, vol. 84, no. 2, pp. 92-102.

Lu, Y.; Song, C.; Jia, Y.; Xia, B.; Ge, Z. et al. (2015): Analysis and numerical simulation of hydrofracture crack propagation in coal-rock bed. *Computer Modeling in Engineering and Sciences*, vol. 105, no. 1, pp. 69-86.

Qin, Y.; Moore, T. A.; Shen, J.; Yang, Z.; Shen, Y. et al. (2018): Resources and geology of coalbed methane in China: a review. *International Geology Review*, vol. 60, no. 5-6, pp. 777-812.

Song, C.; Elsworth, D. (2018): Strengthening mylonitized soft-coal reservoirs by microbial mineralization. *International Journal of Coal Geology*, vol. 200, pp. 166-172.

Song, C.; Lu, Y.; Tang, H.; Jia, Y. (2016): A method for hydrofracture propagation control based on non-uniform pore pressure field. *Journal of Natural Gas Science and Engineering*, vol. 33, pp. 287-295.

Surjaatmadja, J. B.; Grundmann, S. R.; McDaniel, B.; Deeg, W. F. J.; Brumley, J. L. et al. (1998): Hydrajet fracturing: an effective method for placing many fractures in openhole horizontal wells. *SPE International Oil and Gas Conference and Exhibition in China, Society of Petroleum Engineers*, SPE-48856-MS.

Tang, C. A; Kou, S. Q. (1998): Crack propagation and coalescence in brittle materials

under compression. *Engineering Fracture Mechanics*, vol. 61, no. 3-4, pp. 311-324.

Tang, C. A.; Tham, L. G.; Lee, P. K. K.; Yang, T. H.; Li, L. C. (2002): Coupled analysis of flow, stress and damage (FSD) in rock failure. *International Journal of Rock Mechanics and Mining Sciences*, vol. 39, no. 4, pp. 477-489.

Tang, Z.; Yang, S.; Zhai, C.; Xu, Q. (2018): Coal pores and fracture development during CBM drainage: their promoting effects on the propensity for coal and gas outbursts. *Journal of Natural Gas Science and Engineering*, vol. 51, pp. 9-17.

Wang, J.; Elsworth, D. (2018): Role of proppant distribution on the evolution of hydraulic fracture conductivity. *Journal of Petroleum Science and Engineering*, vol. 166, pp. 249-262.

Wang, G.; Li, W.; Wang, P.; Yang, X.; Zhang, S. (2017a): Deformation and gas flow characteristics of coal-like materials under triaxial stress conditions. *International Journal of Rock Mechanics and Mining Sciences*, vol. 91, pp. 72-80.

Wang, G.; Wu, M.; Wang, R.; Xu, H.; Song, X. (2017b): Height of the mining-induced fractured zone above a coal face. *Engineering Geology*, vol. 216, pp. 140-152.

Xu, T.; Tang, C. A.; Yang, T. H.; Zhu, W. C.; Liu, J. (2006): Numerical investigation of coal and gas outbursts in underground collieries. *International Journal of Rock Mechanics and Mining Sciences*, vol. 43, no. 6, pp. 905-919.

Yang, T. H.; Tham, L. G.; Tang, C. A.; Liang, Z. Z.; Tsui, Y. (2004): Influence of heterogeneity of mechanical properties on hydraulic fracturing in permeable rocks. *Rock Mechanics and Rock Engineering*, vol. 37, no. 4, pp. 251-275.

Zhang, Q.; Ma, D.; Wu, Y.; Meng, F. (2018): Coupled thermal-gas-mechanical (TGM) model of tight sandstone gas wells. *Journal of Geophysics and Engineering*, vol. 15, no. 4, pp. 1743-1752.